How to Cite:
Soni, D., & Shrivastava, P. (2022). Development and evaluation of ligand Binded Phytoactive extract loaded SLN for brain targeting. *International Journal of Health Sciences*, *6*(S6), 3920–3939. https://doi.org/10.53730/ijhs.v6nS6.10212

Development and evaluation of ligand Binded Phytoactive extract loaded SLN for brain targeting

Deependra Soni
Faculty of Pharmacy, Kalinga University, Naya Raipur, Raipur
*Corresponding author email: deependra.soni@kalingauniversity.ac.in

Pranjul Shrivastava
Faculty of Pharmacy, Kalinga University, Naya Raipur, Raipur

Abstract---Drug delivery to the brain is the process of passing therapeutically active molecules across the Blood Brain Barrier for the purpose of treating brain disease. This is a complex process that must take into account the complex anatomy of the brain as well as the restrictions imposed by the special junctions of the Blood Brain Barrier. In response to the insufficiency in conventional delivery mechanisms, aggressive research efforts have recently focused on the development of new strategies to more efficiently deliver drug molecules to the CNS.The objective of present work deals with the preparation ofdevelopment and evaluation of ligand binded phytoactive extract loaded SLN for brain targeting.Solid lipid nanoparticles (SLNs) are spherical solid lipid nanoparticles in nanorange, easiy dispersibe in water or in aqueous surfactant solution present themselves as suitable candidate for drug delivery to the brain. These nanoparticles can easily penetrate blood brain barrier (BBB) and has good stability & lesser toxicity. In present work, phytoactive loaded SLN conjugated with lactoferrin was prepared by solvent evaporation method and was characterized for particle size, drug loading entrapment, ligend binding & targetability to brain cells. The result of the study showed that the prepared lactoferrin conjugated SLN of phytoactive has targetability towards brain cells. The prepared SLN showed particle size in the range of 112.58± 0.027 to 120± 0.156 nm with a zeta potential at a range of 23± 0.56 mV to 27 ± 0.19 mV. The drug entrapment efficiency was around 84.3± 1.09%. The lactoferrin conjugated Phyto extract loaded SLN showed higher uptake by brain cell *in vitro*.

Keywords---drug delivery, blood brain barrier, solid lipid nanoparticles, lactoferrin conjugated, ligand binded, photoactive extract.

Introduction

Drug delivery to the brain is the process of passing therapeutically active molecules across the Blood Brain Barrier for the purpose of treating brain disease. This is a complex process that must take into account the complex anatomy of the brain as well as the restrictions imposed by the special junctions of the Blood Brain Barrier[1].In response to the insufficiency in conventional delivery mechanisms, aggressive research efforts have recently focused on the development of new strategies to more efficiently deliver drug molecules to the CNS.Various routes of administration as well as conjugation of drugs, e.g. with liposome and nanoparticles are considered. Solid lipid nanoparticles (SLNs) which consist of spherical solid lipid nanoparticles in the nanometer range, which are dispersed in water or in aqueous surfactant solution may be a suitable option for drug delivery to the brain after considering the success of the nanoparticles to pass through the BBB and their limitations such as toxicity and stability. The SLNs has the potential to carry both lipophilic and hydrophilic drugs. Solid lipid nanoparticles (SLN) delivery can be an ingenious way to administer molecules into the brain by possibly overcoming or alleviating the solubility, permeability and toxicity problems linked with the respective drug molecules [2].SLN are taken up readily by the brain due to their lipidic nature. Although, SLN deliver comparatively high amount of drug to brain but they show extrapyrimidal side effects because of their non-specificity.

Astragalosides is used in the treatment of many types of cancer but its entry and uptake into the brain is limited due to the p-gp efflux at BBB. Being lipophilic drug can be easily encapsulated in the SLN matrix. Drug binded-SLN is used to improve drug delivery to brain and reported increased drug concentration of these SLN in brain. Lactoferrin (Lf), a glycoprotein belonging to the transferrin (Tf) family, consists of a polypeptide chain of about 690 amino acids folded into two globular lobes and each of which contains one iron-binding site. Lf has been localized in human brain to neurons, glial cells and microvasculature [3]. Lf receptor (LfR) has been demonstrated to exist on the BBB in different species and is involved in Lf transport across the BBB in vitro and in vivo receptor mediated transcytosis. LFs is an iron- binding protein involved in host defense against infection and severe inflammation, it accumulates in the brain during neurodegenerative disorders [4]. Lf binding sites present in brain endothelial capillary cells. Brain endothelial capillary cells prevent circulating compounds, including their therapeutic drugs, from reaching the brain by passive transport or through the Para cellular route. Lf easily and effectively transfers the BBB through the transcytosis mechanism of brain endothelial capillary cells [5].

Material and Method

Materials

Glycerol monostearate, Polyethylene glycol400 and other excipients received from college laboratory grade. lactoferrin was purchased from sigma Aldrich.

Method of preparation

Method of preparation of blank SLN: By using solvent evaporation/emulsification method

GMS- 85mg (glycerol mono stearate), SA -15mg (stearic acid), SL-35mg (soy-lecithin) and Drug (*Astragalus membranaceous)* were dissolved in 2ml of chloroform to get lipid phase in organic solvent.Aqueous phase was prepared by dissolving 150mg Tween 80 in 10ml of de-ionized water [18].Lipid phase containing organic solvent was added to aqueous phase and homogenized for 5min at 12000rpm.Emulsion, thus obtained, was sonicated for 15min.The nanoemulsion was kept under stirring for 3h to get drug-loaded SLN and then lyophilized for one hour [19].

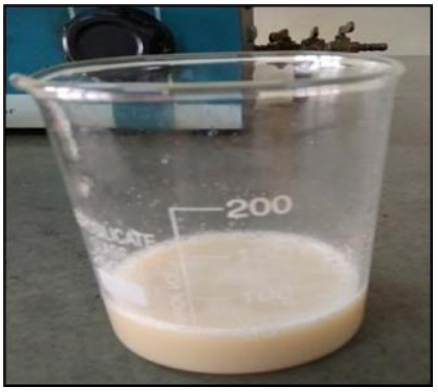

Fig 1. Prepared SLN

Method of preparation of drug loaded SLN

GMS- 85mg (glycerol mono stearate), SA -15mg (stearic acid), SL-35mg (soy-lecithin) and Drug (*Astragalus membranaceous)* were dissolved in 2ml of chloroform to get lipid phase in organic solvent.Dissolve the drug in the lipid phase.Aqueous phase was prepared by dissolving 150mg Tween 80 in 10ml of de-ionized water.Lipid phase containing organic solvent was added to aqueous phase and homogenized for 5min at 12000rpm.Emulsion, thus obtained, was sonicated for 15min [20].The nanoemulsion was kept under stirring for 3h to get drug-loaded SLN and then lyophilized for one hour.

Method of conjugation of lactoferrin (LF) to SLN

For this, 20mg of Drug-loaded SLN were dispersed in 1ml of phosphate buffer saline, PBS (pH 7.4).The dispersion was kept on gentle stirring for 1h at room temperature.To this, 0.6mg Lf (1mg/ml in PBS, pH 7.4) was added, mixed well and kept for stirring for 4h.Excessive unbound Lfwas removed by centrifugation using high speed refrigerated table top centrifuge at 12000rpm for 30min. The SLN pellets were then lyophilized and lactoferrin (LF) SLN was characterized using various techniques [21].

Evaluation of Solid Lipid Nanoparticles

It is necessity of evaluation of important parameters of SLNs for its quality control. The important parameters which need to be evaluated for the SLNs are–

Evaluation of astragalosides dispersions
Solubility of solid dispersion

- Solubility ofastragaloside was determined in water, ethanol, methanol and DMSO.
- Effect of stirring time on astragaloside loaded solid lipid nanoparticles- Stirring is a magnetic stirrer is very important parameter as it is the only step that incorporates shear in the process. Particle size and entrapment efficiency were estimated at different stirring times ranging from 10 minutes to 4 hours [29].

Measurement of Particle size, Zeta Potential, PDI

The average particle size, PDI, and zeta potential of the phytoactive extract loaded solid lipid nanoparticles were determined using Zetasizer Nanoseries Nano-ZS, Malvern Instruments, Malvern, UK. Dynamic light scattering, DLS, and Laser Doppler Electrophoresis were used for the estimation of particle size and for zeta potential. The samples were place in "folded capillary cells" and results obtained for size, PDI, and zeta potential was recorded. Zeta potential is mainly the surface charge of the nanoparticles and can be amarker of the potential stability over time. Nanoparticles have a normal tendency to aggregate, although charged nanoparticles, with high negative or positive zeta potential, will repeal each other overcoming this problem. As a result, particles can be considered stably dispersed when the total value of zeta potential is higher than 20 mV due to the electrostatic repulsion between the particles, while potentials of 5–15 mV shows in limited flocculation in solution [3].

Entrapment efficiency

The entrapment efficiency can be determined by measuring the concentration of the free drug in the dispersion medium. Entrapment efficiency of nanoparticles in different formulation are determined by ultracentrifugation of samples at 10,000 rpm for 30 min. The amount of freeastragalosides was determined in clear supernatant by UV spectrophotometry at 227nm using supernatant of non-loaded (blank) nanoparticles as basic correction. The entrapment efficiency (EE) of the process was calculated from equations 1 and 2 indicated below:

$$\text{Entrapment efficiency (EE \%)} = \frac{\text{Total amount of drug} - \text{Free Drug}}{\text{Total Drug}} \times 100$$

Cytotoxicity study

In vitro cytotoxicity of formulations was estimated on U-87 MG cells employing MTT assay. Growth inhibition result on U-87 MG cells were observed in both

groups. The IC50 values of the ASG, SLN (SLN – ASG-loaded unconjugated solid lipid nanoparticles,)and C-SLN (C-SLN – lactoferrin conjugated ASG-loaded solid lipid nanoparticles). on U-87 MG cells were found to be 0.857 ± 0.009, 0.792 ± 0.027 and 0.476 ± 0.009 mg/ml, respectively. The IC50 of the ASG-loaded conjugated SLN (C-SLN) were lower than pure ASG, indicating ASG-loaded C-SLN were more efficient to mediate cytotoxic effect than ASG**.** Higher cell toxicity and lower IC50 of C-SLN formulation in the cells indicate that conjugating Lf on the surface of SLN increases the targeting efficiency of ASG in mentioned cells.

Ligand-receptor binding assay

Cytotoxicity was also studied after saturating LfR present in U-87 MG cells with free Lf. For competitive ligand-receptor binding assay, 1x 10^4 cells were co-incubated with 800 M excess of Lf for 30 min followed by washing and treatment with formulations and positive control astragalosideswith series of concentrations for 48 h at 37 °C in DMEM with 10% FBS medium. Thereafter, MTT assay was perfomed as described above. Obtained IC50 values from competitive ligand-receptor binding assay were compared with previously obtained IC50 values of MTT assay.

Drug content uniformity

SDs equivalent to 10 mg of astragalosidewere weighed accurately and dissolved in methanol, suitably diluted and the drug content was analyzed at 425 nm using Shimadzu UV spectrophotometer in triplicate [22].

TLC studies

Interaction of the drug with the carrier was studied by TLC method. Chloroform and methanol in 9.25:0.75 ratios was used as mobile phase and Silica gel G was Stationary phase. The spots were detected under UV light as well as fluorescence light and Rf values were noted [23].

FTIR studies

In this study, potassium bromide disc method was employed. Pure drug and solid dispersions were subjected to FTIR studies. The powdered sample was intimately mixed with IR grade potassium bromide. The mixture was then compressed into transparent disc under high pressure using special dies. The disc was placed in FTIR spectrophotometer using sample holder and spectrum was recorded [24].

Scanning Electron Microscopy (SEM) studies

Pure drug as well as solid dispersions was sputtered coated using pelco gold palladium coaters. The surface morphology of the layered sample was examined using SEM. The sample was placed in an evacuated chamber and scanned in a controlled pattern by an electron beam. Interaction of the electron beam with the specimen produces a variety of physical phenomenon that detected, are used to form images and provide information about the specimens [25].

X-ray diffraction studies

Crystalline compounds give characteristic X-ray diffractogram. This pattern of diffraction is useful for the identification of compound. Quantitative analysis of X-ray powder diffraction technique is a measurement of a series of d spacing, the interplanar spacings from the position of the diffraction peaks. The diffraction angle is recorded in terms of 2θ and all 2θ values are readily converted to d-values expressed in angstroms units for a given wave length of X rays [26].The sample was rotated during the data collection to reduce orientation effects, and the data was recorded using a curved photosensitive detector. The X ray was measured in the range of 2θ=10 to 60 at steps of (100) at ambient temperature.

Differential Scanning Calorimetry

DSC thermograms were recorded using differential scanning calorimeter. Approximately 2- 5 mg of sample was heated in an open aluminium pan from 30-3000C at a scanning rate of 100 C/ min under a stream of nitrogen [27].

***In vitro* dissolution studies of optimized solid dispersions**

In vitro release of astragalosides from the SLN and C-SLN were passed out using the dialysis bag diffusion technique [35]. The release media was PBS (pH 7.4) containing 0.5% Tween 80 (w/v) to maintain the sink condition. SLN, C-SLN and drug suspension (equivalent to 1 mg of Astragalosides) were put into the pre-swollen dialysis bags (14 kDa molecular weight cut off) and was immersed in 50 ml of release medium in separate beakers, placed in a horizontal shaker bath maintained at 37 ± 0.5 °C and 100 rpm. At fixed time intervals, samples were withdrawn and replaced with fresh PBS medium. The concentration of astragalosides in the samples withdrawn from the incubation medium was analysed by HPLC as explained previously. Data obtained in triplicate were analysed graphically and percentage cumulative amount of astragalosides released from formulations versus time was plotted

***In vitro* Cellular uptake**

To carry out the cell uptake study, the chemical conjugate of ODA-FITC was synthesized as described by Yuan et al. with modifications [38]. Briefly, ODA was dissolved in methanol, and same molar amount of FITC under stirring. After 24 h of reaction in darkness, ODA-FITC was mixed with 10-fold volume of distilled water and filtered. Distilled water was used to wash the product five times. The obtained conjugate (OD-FITC) was freeze dried and stored in dark for further use. This prepared fluorescent marker (ODA-FITC) was then incorporated into SLN for evaluating cellular uptake of SLN. Supernatant of ODA-FITC incorporated lipidic formulations (SLN and C-SLN) was used to check the degree of incorporation of ODA-FITC into these formulations. Around 20% ODA-FITC was found entrapped in the nanoparticles. U-87 MG cells were seeded on 24-well plate at a density of 5 x 10^4 cells/well in DMEM media and were allowed to adhere for 24 h. After 24 h, the cells were incubated with fluorescent dye (ODA-FITC) labelled formulations for 2 h. Phase contrast and fluorescent images were taken with digital camera (Nikon, Tokyo, Japan). Finally, to quantify the cell uptake, the media was removed

and cells were washed twice with PBS for 2 h. Cell lysis was carried out using Triton X-100. The cell uptake was quantified by measuring the fluorescence in the cell lysate.

Stability Study

A stability study was also carried out to assess the stability of astragalosidesloaded lactoferrin nanoparticles. For this purpose, samples were put in borosilicate glass vials and stored at room temperature, in a refrigerator (5 ± 1°C), and 45 ± 1°C (75% relative humidity) in the stability chamber. Samples were analyzed at the intervals of 0, 7, 14, 21, 28, 35, and 45 days for their changes in physical appearance and for the drug content.

Plasma Concentration

In-vivo studies were performed on adult Wistar albino rats. A protocol for animal studies was approved by Institutional Animal Ethics Committee (IAEC) and Committee for the Purpose of Control and Supervision of Experiments on Animals (CPCSEA). Animals were housed in polypropylene rat cages. Rice husk was used as the bedding material. Laboratory rat pellet feed and pure drinking water were supplied ad libitum. The rats were divided into two groups. Group I (test group) consisting of 6 animals were administered with a total volume of 0.25 mL of the developed SLN formulation (equivalent to 0.06 mg efavirenz), divided into five small volumes of 0.05 mL each administered within a 5-minute interval intranasally [34, 39]. The second group (standard) consisting of 6 animals were given the marketed formulation—EFAVIR—efavirenz capsules IP orally (powder equivalent to 25 mg efavirenz from capsule dispersed in 1 mL water). The plasma samples from each animal were collected and the animals were sacrificed by an overdose of pentobarbital sodium at 24 hours. The brains were isolated, weighed, homogenized in PBS pH 6.4 at 5000 rpm using Silent Crusher M homogenizer (Heidolph, Germany), and centrifuged and the supernatants were collected for determination of drug concentration [15]. The amount of drug in plasma and the brain homogenate were determined by the method developed and validated for estimation of efavirenz in plasma using HPLC (unpublished work). The lower limit of quantificationfor the HPLC method in detecting the drug in plasma was 0.05 μg/mL. Tenofovir disoproxil fumarate was used as internal standard. Brain : Plasma ratio, bioavailable fraction, and relative bioavailability were calculated using the formula-

$$\text{Brain : plasma} = \frac{\text{Conc. of drug in brain}}{\text{Conc. of drug in plasma}},$$

$$\text{Bioavailable fraction} = \frac{\text{Bioavailable dose}}{\text{Administered dose}}$$

$$\text{Relative bioavailability} = \frac{\text{Systemic availability of drug}}{\text{Systemic availability of an oral standard of same drug.}}$$

Results and Discussion

Background information such as chemical name, structure, solvent of recrystallization, purity, therapeutic category, appearance, color and Odour studied according to literature review.

Solubility

Effect of stirring time on astragaloside loaded solid lipid nanoparticles

Stirring is a magnetic stirrer is very important parameter as it is the only step that incorporates shear in the process. Particle size and entrapment efficiency were estimated at different stirring times ranging from 10 minutes to 4 hours. The results at different stirring times are summarized in below table. Stirring for more than 1 hour leads to high variability in the test results between different batches. Though the particle size remains below 300nm, the standard deviation within 3 replicate batches remains on higher side. Stirring for longer time may lead to particle aggregation which may be contributing to higher variability. Stirring for 30 minutes was considered to be optimum to yield SLNs with desired particle size and entrapment efficiency.

Table 1
Effect of stirring time on astragaloside loaded solid lipid nanoparticles

Stirring time	Particle size distribution (nm)	Entrapment efficiency (%)
10 min.	799.3±76.0	20.1±10.3
30 min.	112.1±13.5	71.2±1.8
60 min.	154.8±88.9	74.3±2.5
120 min.	154.8±67.1	68.6±13.4
180 min.	244.8±87.6	43.8±34.4
240 min.	278±17.1	65.1±22.6

Measurement of Particle size, Zeta potential & PDI

Particle size and polydispersity characterization of ASG-loaded SLNs can be seen in Table 2, where particle size, PDI and zeta potential are presented. Regarding the particle size, all nanoparticles showed an homogenous size distribution with a mean diameter of about 155 nm and no statistically significant differences between them were observed ($P > 0.05$), suggesting that astragaloside incorporation does not directly influence the nanoparticles size (Table 2). In relation to PDI, the values obtained were lower than 0.2 for all nanoformulations (Table 2), suggesting that the nanoparticles were in a state of acceptable monodispersity distribution, with low variability and no aggregation. All formulations presented (Table 2) have a negative average zeta potential between −10 and −15 mV, regardless of astragalosideincorporation on lipid nanoparticles ($P > 0.05$). Therefore, it is essential to perform a stability study to ascertain the formulations stability over time, once the zeta potential is notvery high and it may lead to the occurrence of some flocculation and aggregation between the nanoparticles. The zeta potential of the SLNs developed did not significantly

change over time. Therefore, despite the initial zeta potential value is not as high as desired, no tendency for zeta potential to change was found during storage conditions, indicating that the SLNs developed will be stable at least for 6 months.

Table 2
Data of particle size, zeta potential & PDI

Formulation no.	Particle size (nm)	Zeta potential (mV)	PDI
F1	566.4 ±7.4	23± 0.56	0.494 ±0.2
F2	891.1± 8.1	24± 0.21	0.363 ±0.3
F3	628.3 ±9.3	26± 0.23	0.488± 0.3
F4	697.4 ±9.7	25 ±0.07	0.511± 0.4
F5	620.3± 8.5	27 ±0.19	0.500 ±0.3

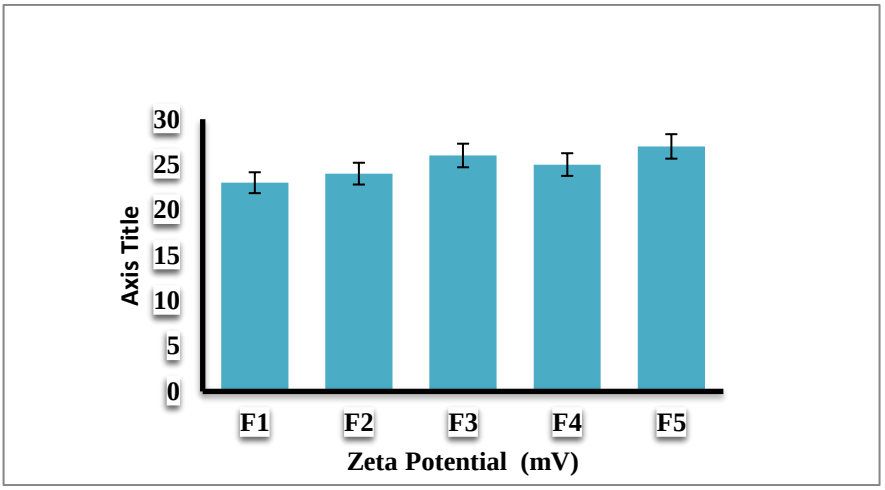

Figure No. 2

Entrapment efficiency

Entrapment efficiency means that the amount of drug in the precipitate did not change via different formulations. But, for constant amount of entrapped drug, upon increasing surfactant concentration the number of excipients increases, which results in reduced drug loading.

Table. 3
% drug entrapment efficiency

Formulation No.	Entrapment efficiency (%)
F1	50.1±10.3
F2	71.2±1.8
F3	74.3±2.5
F4	81.6±13.4
F5	84.8±34.4

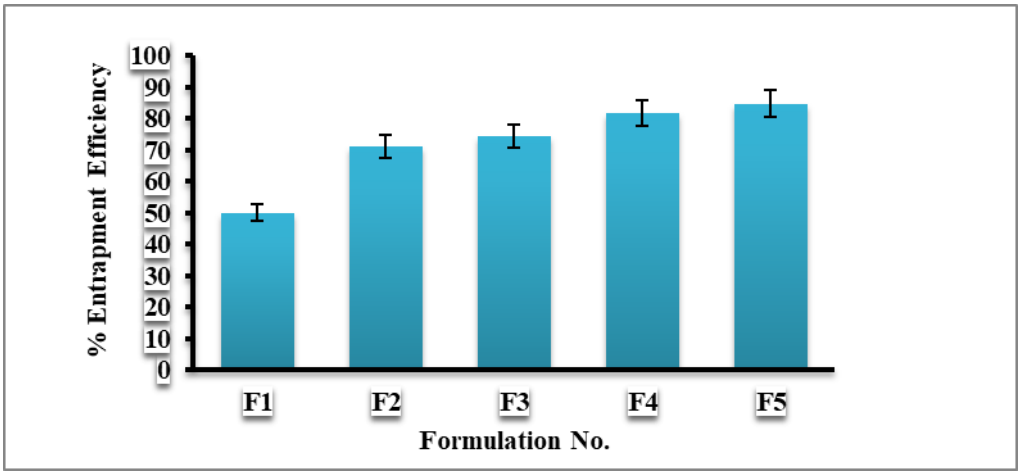

Figure No. 3 % Drug Entrapment Efficiency

Percentage Entrapment efficiency was found to be highest for F5 formulation which is 84.8% whereas the lowest entrapment of drug was found to be for F1 having 50.1%.

Table 4
Percentage drug Content of selected solid dispersions

S. No.	Method	Code	% Drug content ± S.D
1.	SDHM	H3	98.82 ± 0.10
2.	SDSEM	S3	97.53 0.12

Table 3: Effect of stirring time on astragaloside loaded solid lipid nanoparticles:

Ligand-receptor binding assay

Mechanism involved in internalisation of C-SLN was studied by competitive ligand-receptor binding assay. IC50 values were significantly increased (p50.001) after saturation of LfR with free Lf. IC50 of C-SLN was increased to 0.712 ± 0.039 mg/ml after saturation of U-87 MG cell line with free Lf (Figure 3a). This increase in IC50 was attributed due to blockage of LfR by free Lf, hence hindering uptake of C-SLN. Once all the receptors are saturated with free ligand, conjugated Lf on lipidic nanoparticle becomes ineffective. Hence, providence of C-SLN will be decided on its physical properties, which are similar to SLN. This study delineated the importance of Lf conjugation on the surface of SLN which aids in internalisation of C-SLN through LfR in brain tumour cells.

Drug - polymer compatibility studies by FTIR

Fourier transform Infrared spectrometer study was conducted to check the

compatibility among formulation's components.The FTIR spectrographs of pure drug, excipients and solid dispersions indicated no interaction of astragaloside with carriers in our study. The chemical structure of astragaloside shows the peaks at 3500-3300 cm-1, 1625 – 1640 cm-1 and 1520 – 1400 cm-1 in the FTIR spectrum were observed in both pure drug as well as in solid dispersion (H3) indicating no interaction between drug and polymer.

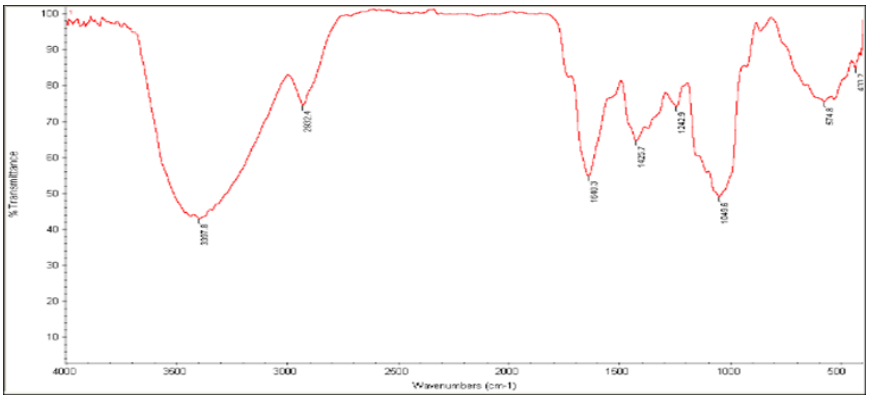

Fig 4: FTIR analysis for blank SLN

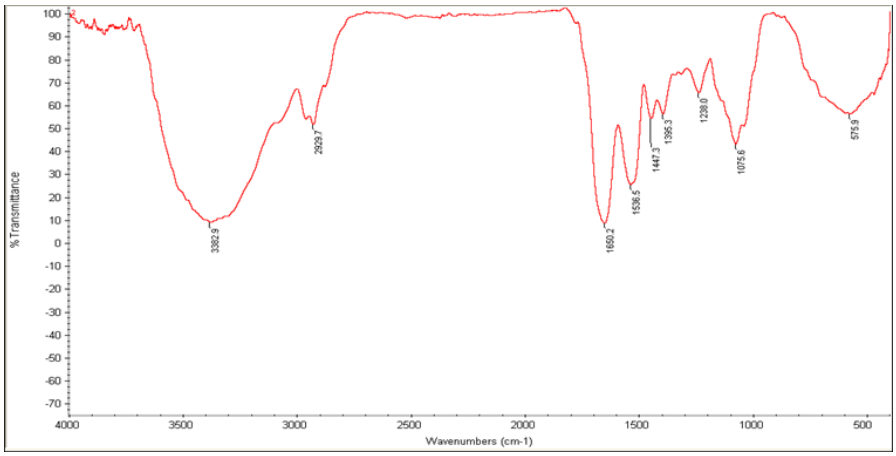

Fig 5. FTIR analysis for drug loaded SLN

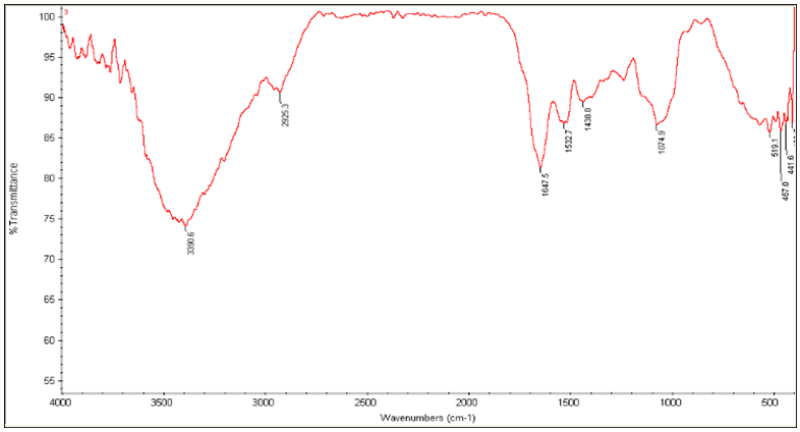

Fig 6. FTIR analysis for ligand binded SLN

Scanning Electron Microscopy (SEM) studies

SEM studies of pure drug were carried out in order to analyze surface morphology of pure drug as well as solid dispersions. Pure drug particles were spherical in shape while solid dispersion obtained from solvent evaporation method (S3), the particles was plane and uniform indicating that drug is soluble in the PEG 6000 and converted into amorphous state and the drug particles and the carrier were adsorbed on the adsorbent. SEM studies of pure astragaloside and solid dispersions were carried out in order to analyze the changes in surface morphology of pure drug as well as solid dispersions. Pure drug particles were spherical in shape while solid dispersion obtained from hot melt method were plane (wavy) and uniform indicating that drug is soluble in the PEG 6000 and converted into amorphous state which might be the reason for improvement of solubility. In case of solid dispersion obtained by solvent evaporation method, the particles were roughly spherical and the drug particles and the carrier were adsorbed on the adsorbent.

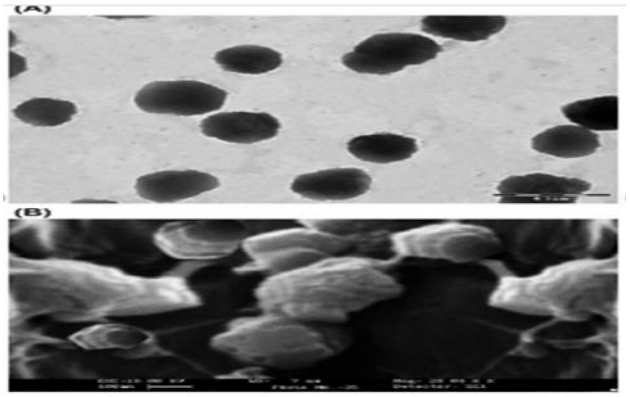

Fig 7. SEM analysis of drug binded SLN

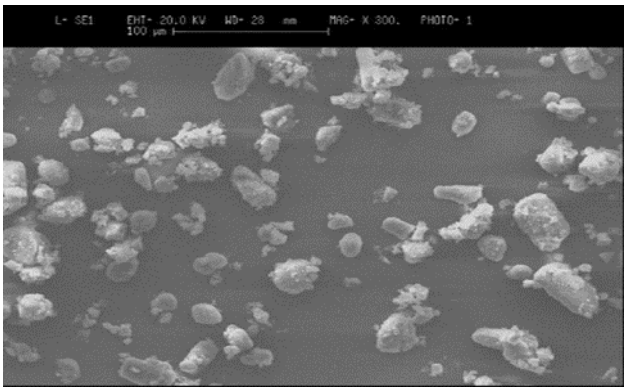

Fig 8. SEM analysis of ligand binded SLN

X-ray diffraction studies

X- ray diffraction studies of pure astragaloside and its solid dispersions were investigated from the angle of 10 ^{0} to 70 ^{0}. The intensity vs angle (2θ in degrees) was plotted, which showed the decrease in intensities of drug in solid dispersion.X ray diffraction studies of pure astragaloside and its solid dispersions were investigated from the angle of 10 ^{0} to 70 ^{0}

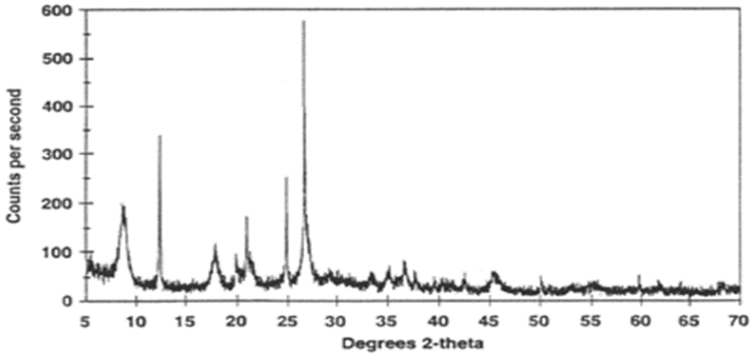

Figure No. 9. XRD of blank SLN

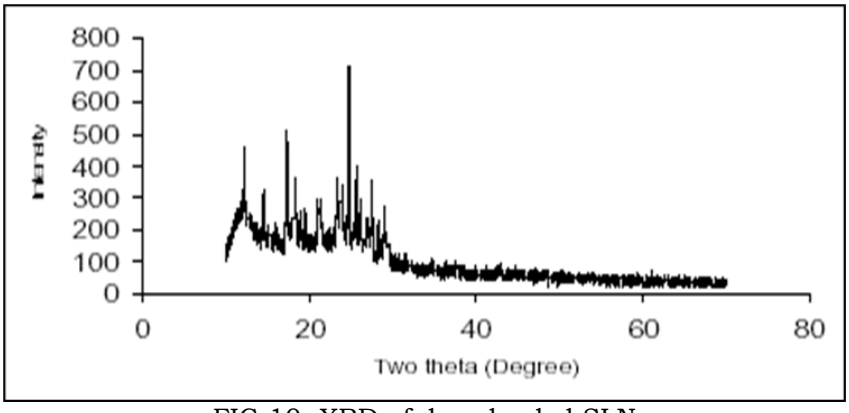

FIG 10. XRD of drug loaded SLN

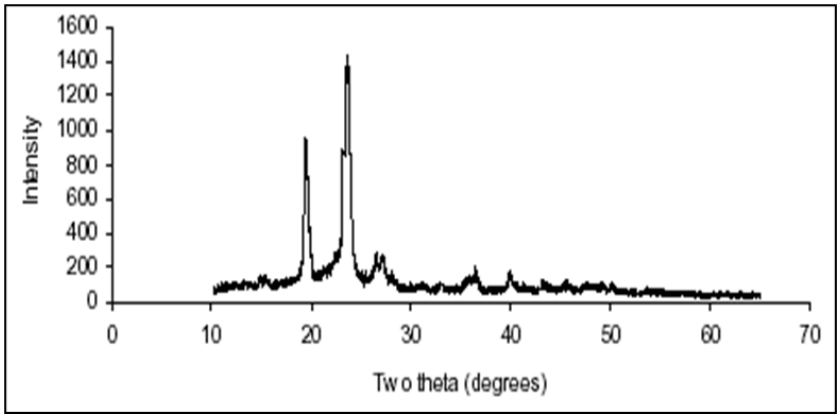

Fig 11. XRD of ligand conjugated SLN

DSC of astragaloside solid dispersions

The DSC curve of pure astragaloside showed a single sharp endothermic peak at 1800 C. All solid dispersion systems showed no endothermic peaks ofastragaloside. These findings may be due to the formation of an amorphous solid solution which has been known to cause an increase in drug dissolution.The DSC thermograms of astragaloside, PVP K-30, PEG 6000, and solid dispersions of astragaloside were illustrated. The DSC curve of pure astragaloside showed a single sharp endothermic peak at 1800 C. All solid dispersion systems showed no characteristic endothermic peaks of astragaloside which might be due to the formation of an amorphous solid solution which has been known to be the contributing factor for enhanced solubility and dissolution profile.

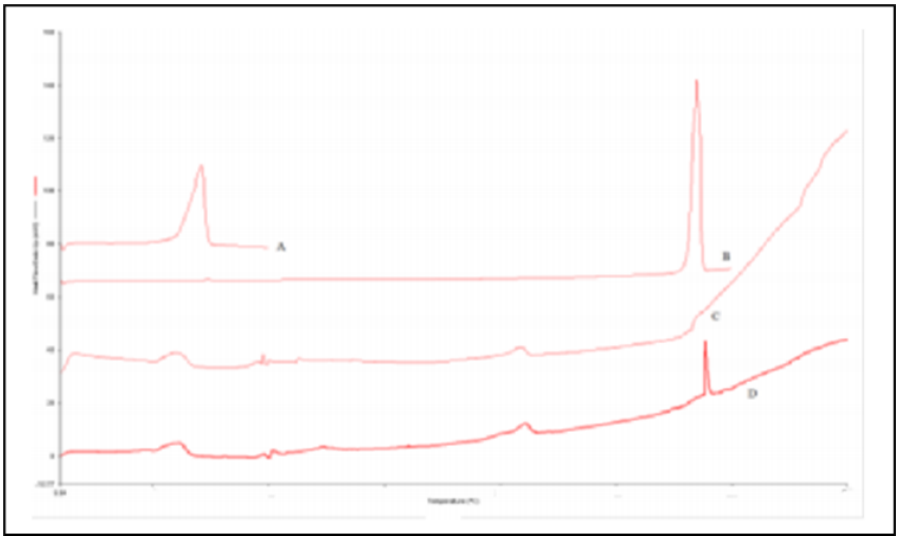

FIG 12. DSC OF (A) Blank SLN, (B) Drug Loaded SLN, (C) Ligand Binded SLN

***In vitro* dissolution studies of optimized solid dispersions**

The *In vitro* drug release profiles are represented as cumulative percentage drug released with respect to time. Considerable difference was observed in the release of Astragalosidefrom C-SLN compared to SLN and Pure Astragaloside. C-SLNexhibited more than 95% release in 12 h whereas drug release from lipidic nanoparticles was slow. SLN exhibited approximately 47% release and pure ASG also exhibited approximately 22% release of astragaloside in PBS (pH 7.4) in 24 h (Figure 13). Conjugation process is responsible for the loss of drug present on the surface of pure ASG. Kumar et al. Suggested due to surface modification with ligand, particle size of conjugated SLN was increased and that showed in increased distance between the core and the surface of nanoparticles which caused less release of drug from pure ASG as compared to that from SLN and C-SLN suspension [15]. As well, surface conjugation lead to increase in size of ASG can slower the release rate because there is less total surface area and the release rate is proportional to particle surface area [46]. Their findings supported the present results.

Table 5
In vitro Drug Release profile

Time (h)	Cumulative percentage release		
	C-SLN	SLN	ASG
0	0	0	0
5	21.01±0.03	8.06±0.63	2.01±0.32
10	46.21±0.48	21.32±0.34	15.04±0.19
15	71.04±0.02	29.07±0.51	20.04±0.24
20	88.12±0.10	38.09±0.31	20.13±0.62
25	93.26±0.04	47.03±0.34	21.03±0.04
30	98.04±0.23	48.05±0.12	21.09±0.39

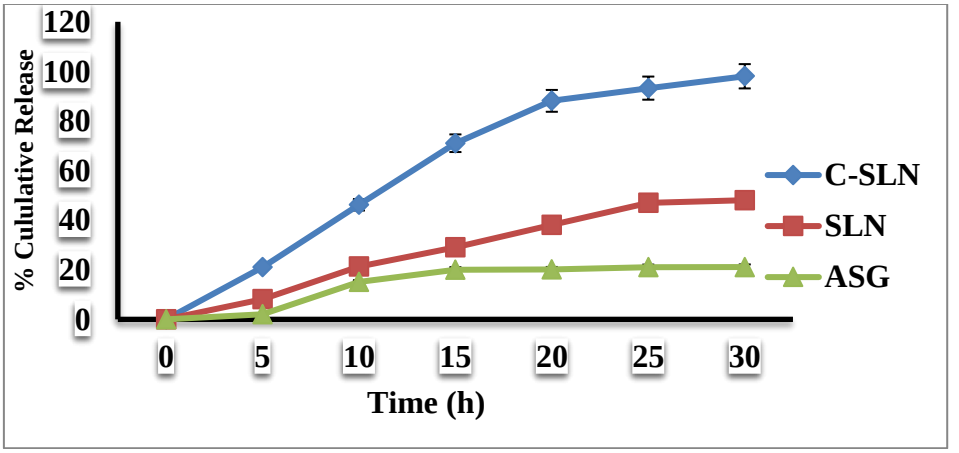

Figure. No. 13

In vitro release profile of drug and lipidic nanoparticles in PBS (pH 7.4). Considerable difference was observed in the release of drug from C-SLN as

compared to SLN and ASG. Data evidencing sustained release of C-SLN from SLN and ASG formulations as compared to C-SLN. Data presented as mean ± SD, n ¼ 3. (SLN – ASG-loaded unconjugated solid lipid nanoparticles, C-SLN – lactoferrin conjugated ASG-loaded solid lipid nanoparticles).

***In vitro* Cellular uptake**

Fluorescein isothiocyanate isomer I (FITC) tagged lipidic nanoparticles have shown increased cellular uptake compared to FITC (Control Marker). Quantitative cellular uptakes of FITC, FITC tagged SLN and FITC tagged conjugated Lf-SLN after 2 h were determined to be 0.227 ± 0.10, 7.49 ± 0.33 and 20.9 ± 5.44%, respectively (Figure 3b). Fluorescent images of uptake studies depicted that Lf facilitated in increasing the internalisation of SLN in these cells (Figure 4). This higher uptake substantiated the higher cytotoxicity of C-SLN in U-87 MG cells.

Stability Study

The SLN were taken and observed their physical properties at an interval 0f 7, 14,21,28,35 and 45 days. No change was observed in their physical appearance. Colour remains the same. The drug content remains unchanged in 5 ± 1°C and room temperature.

Table 6
Drug content in stability Studies

SN	Sampling Interval days	Drug content		
		5 ±1 °C	Room Temperature	45± 2 °C
1.	7	100	100	100
2.	14	99.4	99.5	99.5
3.	21	99.1	98.4	98.5
4.	28	98.8	97.4	87.4
5.	35	98.5	96.5	78.9
6.	45	98.1	94.7	74.3

Plasma Concentration

The concentration of the drug in plasma and brain was determined after intranasal administration of the developed solid lipid nanoparticulate formulation (equivalent to 0.06 mg efavirenz) and was compared with the concentration of the drug achieved in plasma and brain with the oral administration of the marketed formulation (25 mg powder from capsule dispersed in 1 mL water). The ratio of drug concentration in brain to plasma of 15.61% was achieved with the developed formulation in comparison to 0.104% observed with the oral standard indicating the 150 times more brain targeting efficiency of the formulation through intranasal route which may be because of direct nose-to-brain delivery achieved through integrated olfactory and trigeminal route.The drastic reduction in brain to plasma drug concentration with oral route may be due to first-pass effect, drug degradation in GIT, and presence of BBB. The bioavailable fraction of the drug was calculated to be 0.2454 with the developed formulation while it was found to

be 0.0035 with the standard. Relative bioavailability was determined to be 70.11 with the developed formulation indicating 70 times better absorption potential of the efavirenz loaded SLN dispersion in comparison to the orally administered drug powder. This may be attributable to systemic absorption of some amount of drug when administered intranasally. This may be higher in comparison to the orally administered drug due to avoidance of first-pass metabolism, degradation of drug in GIT, and so forth. The results were found to be in accordance with the similar investigations with different drugs for brain targeting.

Conclusion

In present work, drug loaded SLN and lactoferrin conjugated drug SLN was prepared by solvent evaporation method. Enhancement of drug uptake into brain is a delicate task in the treatment of several neurological disorders. It is a matter of discussion that why lactoferrin conjugated SLN has not been tried for active targeting to brain tumor, in spite of their higher stability, biocompatibility and higher drug payload. Hence, in present investigation, drug-loaded SLN were prepared using emulsification and solvent evaporation method with narrow size distribution and high drug loading efficiency. LfR exist not only on the BBB in different species but also on the cells surface of glioblastomas. Based on this priori, SLN were surface modified with Lf to improve the brain uptake of SLN. Cytotoxicity studies revealed enhanced efficacy of C-SLN. Significantly higher uptake and ligand receptor saturation studies further substantiated the role of conjugating Lf on lipidic nanoparticles.

References

1. Ghada Abdelbary and Rania HF. Nanoparticles: A Review. AAPS Pharm. Sci. Tech 2009; 10(1): 51-63.
2. Reddy LH, Murthy RS. Etoposide-loaded Nanoparticles made from Glyceride Lipids: Formulation, Characterization, in-vitro drug release and stability evaluation. AAPS Pharm Sci Tech 2005; 6: E158-E166. http://dx.doi.org/10.1208/pt060224.
3. Jenning V, Gohla SH, Lippacher A. Medium scale production of Solid Lipid Nanoparticles (SLN) by high Pressure Homogenization. Journal of Microencapsulate 2002; 19: 1-10. http://dx.doi.org/10.1080/713817583.
4. Swathi, G., Prasanthi, N.L., Manikiran, S.S., Ramarao, N. (2010). Solid lipid nanoparticles: colloidal carrier systems for drug delivery. IJPSR 1(12): 01-16.
5. Sarathchandiran, I. (2012). A Review on Nanotechnology in Solid Lipid Nanoparticles IJPDT 2(1): 45-61.
6. Mulla, J.S., Khazi, I.M., Jamakandi, V.G. (2010). Solid lipid nanoparticles: Potential applications IJNDD 2(3): 82-87.
7. Rupenagunta, A., Somasundaram, I., Ravichandiram, V., Kausalya, J., Senthilnathan, B. (2011). Solid lipid nanoparticles- A versatile carrier system. J Pharm Res. 4(7): 20692075.
8. Rupenagunta, A., Somasundaram, I., Ravichandiram, V., Kausalya, J., Senthilnathan, B. (2011). Solid lipid nanoparticles- A versatile carrier system. J Pharm Res. 4(7): 20692075.

9. Schwarz, C., Mehnert, W., Lucks, J.S., Muller, R.H. (1994). Solid lipid nanoparticles (SLN) for controlled drug delivery I. Production, characterization and sterilization. J Control Release 30(1): 83-96.
10. DeSilva NS, Ofek I, Crouch EC. Interactions of surfactant protein D with fatty acids. Am J Respir Cell Mol Biol 2003;29: 757–70.
11. . Grabarek Z, Gergely J. Zero-length crosslinking procedure with the use of active esters. Anal Biochem 1990;185:131–5.
12. Giljohann DA, Seferos DS, Patel PC, et al. Oligonucleotide loading determines cellular uptake of DNA-modified gold nanoparticles. Nano Lett 2007;7:3818–21.
13. Alyautdin R, Gothier D, Petrov V, et al. Analgesic activity of the hexapeptide dalargin adsorbed on the surface of polysorbate 80coated poly (butyl cyanoacrylate) nanoparticles. Eur J Pharm Biopharm 1995;41:44–8.
14. Tung YT, Chen HL, Yen CC, et al. Bovine lactoferrin inhibits lung cancer growth through suppression of both inflammation and expression of vascular endothelial growth factor. J Dairy Sci 2013; 96:2095–106.
15. Rahul Nair, K.S. Arun Kumar, K. Vishnu priya, M. sevukarajan, Recent Advances in solid liquid nanoparticle based drug delivery system, Journal of Biomedicine Science and research, Volume 3(2), 2011, PP-368-384.
16. Loira-Pastoriza C, Todoroff J, Vanbever R (2014) Delivery strategies for sustained drug release in the lungs. Adv Drug Deliv Rev 75:81–91.
17. K.h Ramteke, S. A. Joshi and S.N. Dhole, A review on solid liquid nanoparticles, IOSR journal of pharmacy, Vol-2, PP.34-44.
18. Cholifah S, Farina Kartinasari W, Indrayanto G. Simultaneous HPLC determination of levamisole hydrochloride and anhydrous niclosamide in veterinary powders, and its validation. J Liq Chromatogr Relat Technol. 2007;31:281–291.
19. Natarajan J, Baskaran M, Humtsoe LC, et al. Enhanced brain targeting efficacy of Olanzapine through solid lipid nanoparticles. Artif Cells Nanomed Biotechnol. 2017;45:364–371.
20. Griffiths PR, De Haseth JA. Fourier transform infrared spectrometry. Hoboken (NJ): John Wiley & Sons; 2007.
21. Fang J-Y, Fang C-L, Liu C-H, et al. Lipid nanoparticles as vehicles for topical psoralen delivery: solid lipid nanoparticles (SLN) versus nanostructured lipid carriers (NLC). Eur J Pharm Biopharm. 2008;70:633–640.
22. Zur M€uhlen A, Schwarz C, Mehnert W. Solid lipid nanoparticles (SLN) for controlled drug delivery-drug release and release mechanism. Eur J Pharm Biopharm. 1998;45:149–155.
23. Yang SC, Lu LF, Cai Y, et al. Body distribution in mice of intravenously injected camptothecin solid lipid nanoparticles and targeting effect on brain. J Control Release. 1999; 59:299–307.
24. Cecchelli R et al 1999 In vitro model for evaluating drug transport across the blood-brain barrier Adv. Drug Deliv. Rev. 36 165–78.
25. Lockman P R et al 2004 Nanoparticle surface charges alter blood-brain barrier integrity and permeability J. Drug Target 12 635–41.
26. Neves A R et al 2013 Novel resveratrol nanodelivery systems based on lipid nanoparticles to enhance its oral bioavailability Int. J. Nanomed. 8 177–87.
27. Hauser P S, Narayanaswami V and Ryan R O 2011 Apolipoprotein E: from lipid transport to neurobiology Prog. Lipid Res. 50 62–74.

28. Kaur I P et al 2008 Potential of solid lipid nanoparticles in brain targeting J. Control. Release 127 97–109.
29. Venishetty VK, Samala R, Komuravelli R, et al. b-Hydroxybutyric acid grafted solid lipid nanoparticles: a novel strategy to improve drug delivery to brain. Nanomedicine 2013; 9:388–97.
30. Anderson BF, Baker HM, Norris GE, et al. Structure of human lactoferrin crystallographic structure analysis and refinement at 2.8 A resolution. J Mol Biol 1989; 209:711.
31. Aisen P, Leibman A. Lactoferrin and transferrin: a comparative study. Biochim Biophys Acta 1972; 257:314–23.
32. Suzuki YA, Lopez V, Lonnerdal B. Mammalian lactoferrin receptors: structure and function. Cell Mol Life Sci 2005; 62:2560–75.
33. Huang RQ, Ke WL, Qu YH, et al. Characterization of lactoferrin receptor in brain endothelial capillary cells and mouse brain. J Biomed Sci 2007; 14:121–8.
34. Ji B, Maeda J, Higuchi M, et al. Pharmacokinetics and brain uptake of lactoferrin in rats. Life Sci 2006; 78:851–5.
35. Hu K, Li J, Shen Y, et al. Lactoferrin-conjugated PEG–PLA nanoparticles with improved brain delivery: in vitro and in vivo evaluations. J Control Release 2009; 134:55–61.
36. Kaur IP, Bhandari R, Bhandari S, Kakkar V. Potential of solid lipid nanoparticles in brain targeting. J Control Release 2008;127:97–109.
37. Trotta M, Debernardi F, Caputo O. Preparation of solid lipid nanoparticles by a solvent emulsification-diffusion technique. Int JPharm 2003;257:153–60.
38. DeSilva NS, Ofek I, Crouch EC. Interactions of surfactant protein D with fatty acids. Am J Respir Cell Mol Biol 2003;29:757–70.
39. Liu Z, Liu D, Wang L, et al. Docetaxel-loaded pluronic p123 polymeric micelles: in vitro and in vivo evaluation. Int J Mol Sci 2011;12:1684–96.
40. Shah R, Eldridge D, Palombo E, Harding I. Optimisation and stability assessment of solid lipid nanoparticles using particle size and zeta potential. J Phys Sci 2014;25:59–75.
41. Alyautdin RN, Petrov VE, Langer K, et al. Delivery of loperamide across the blood-brain barrier with polysorbate 80-coated polybutylcyanoacrylate nanoparticles. Pharm Res 1997; 14:325–8.
42. Alyautdin R, Gothier D, Petrov V, et al. Analgesic activity of the hexapeptide dalargin adsorbed on the surface of polysorbate 80-coated poly (butyl cyanoacrylate) nanoparticles. Eur J Pharm Biopharm 1995; 41:44–8.
43. Lazzari S, Moscatelli D, Codari F, et al. Colloidal stability of polymeric nanoparticles in biological fluids. J Nanopart Res 2012; 14:920–9.
44. Tung YT, Chen HL, Yen CC, et al. Bovine lactoferrin inhibits lung cancer growth through suppression of both inflammation and expression of vascular endothelial growth factor. J Dairy Sci 2013; 96:2095–106.
45. Weiss CK, Kohnle MV, Landfester K, et al. The first step into the brain: uptake of NIO-PBCA nanoparticles by endothelial cells in vitro and in vivo, and direct evidence for their blood-brain barrier permeation. ChemMedChem 2008; 3:1395–403.
46. Garcia-Garcia E, Andrieux K, Gil S, Couvreur P. Colloidal carriers and blood brain barrier (BBB) translocation: a way to deliver drugsto the brain? Int J Pharm 2005; 298:274–92.

47. Wissing SA, Kayser O, Muller RH. Solid lipid nanoparticles for parenteral drug delivery. Adv Drug Deliv Rev 2004; 56:1257–72.
48. Ekambaram P, Sathali AAH, Priyanka K. Solid lipid nanoparticles:
49. A review. Sci Rev Chem Commun 2012; 2:80–102.
50. Trotta M, Debernardi F, Caputo O. Preparation of solid lipid nanoparticles by a solvent emulsification-diffusion technique. Int J Pharm 2003; 257:153–60.
51. Avgoustakis K, Beletsi A, Panagi Z, et al. PLGA-mPEG nanoparticles of cisplatin: in vitro nanoparticle degradation, in vitro drug release and in vivo drug residence in blood properties. J Control Release 2002;79:123–35.
52. Suryasa, W. (2019). Historical Religion Dynamics: Phenomenon in Bali Island. *Journal of Advanced Research in Dynamical and Control Systems*, *11*(6), 1679-1685.
53. Yarmukhamedova, N. F., Matkarimova, D. S., Bakieva, S. K., & Salomova, F. I. (2021). Features of the frequency of distribution of alleles and genotypes of polymorphisms of the gene Tnf-A (G-308a) in patients with rhinosinusitis and the assessment of their role in the development of this pathology. International Journal of Health & Medical Sciences, 4(1), 164-168. https://doi.org/10.31295/ijhms.v4n1.1671